Spacecraft Attitude/Rate Estimation Using Vector-Aided GPS Observations

YAAKOV OSHMAN, Senior Member, IEEE
Technion–Israel Institute of Technology

F. LANDIS MARKLEY
NASA/Goddard Space Flight Center

A sequential filtering algorithm is presented for spacecraft attitude and attitude-rate estimation from Global Positioning System (GPS) differential carrier phase measurements. A third-order, minimal-parameter method for solving the attitude matrix kinematic equation is used to parameterize the state of the filter, which renders the resulting estimator computationally efficient. Borrowing from tracking theory concepts, the angular acceleration is modeled as an exponentially autocorrelated stochastic process, thus avoiding the use of the uncertain spacecraft dynamic model. The new formulation facilitates the use of aiding vector observations in a unified filtering algorithm, which can enhance the robustness and accuracy of the method. Numerical examples are used to demonstrate the performance of the method.

Manuscript received July 1, 1998.

IEEE Log No. T-AES/35/3/06417.

This research was performed while Y. Oshman was on sabbatical with NASA/Goddard Space Flight Center under a National Research Council Associateship.

Authors' addresses: Y. Oshman, Technion–Israel Institute of Technology, Dept. of Aerospace Engineering, Haifa 32000, Israel; F. L. Markley, NASA/Goddard Space Flight Center, Guidance, Navigation and Control Center, Code 571, Greenbelt, MD 20771.

I. INTRODUCTION

Attitude determination methods using Global Positioning System (GPS) signals have been intensively investigated in recent years. In general, these methods can be classified into two main classes. Point estimation algorithms (also called "deterministic" algorithms), in which the GPS measurements at each time point are utilized to obtain an attitude solution independently of the solutions at other time points, were introduced, among others, in [1–3]. Stochastic filtering algorithms, which process the measurements sequentially and retain the information content of past measurements, can produce better attitude solutions by more effectively filtering the noisy measurements. Such algorithms were recently introduced in [4, 5], both of which utilized extended Kalman filtering to sequentially estimate the attitude from GPS carrier phase difference measurements. Both attitude and attitude-rate were estimated, and the filters used the nonlinear Euler equations of motion for attitude propagation. While avoiding the traditional usage of the costly and unreliable gyro package, this approach rendered the resulting filters computationally burdensome and sensitive to inevitable modeling errors [6]. In [4] an attempt was made to robustify the dynamics-based filter by estimating the unknown disturbance torques, modeled as unknown constants.

Although GPS-based attitude estimation methods should enjoy, in principle, the low price and low power consumption of state-of-the-art GPS receivers, and the general availability and robustness of the GPS, these methods are very sensitive to multipath effects and to the geometry of the antennae baseline configuration, and they inherently rely on precise knowledge of the antennae baselines in the spacecraft body frame. On the other hand, methods based on vector observations have reached maturity and popularity in the last three decades. However, as is well known, they too suffer from disadvantages, that can be attributed to the particular attitude sensors on which they are based. Thus, while their readings are relatively noiseless, Sun sensors are very sensitive to Earth radiation effects, and are rendered completely useless during Eclipse. Star trackers can provide accuracy on the order of a few arc-seconds, but are usually extremely expensive. Magnetometers always provide measurements of the Earth magnetic field in spacecraft flying in low Earth orbits, but they are sensitive to unmodeled residual magnetic fields in the spacecraft and to magnetic field model imperfections and variations.

The method presented herein is a sequential estimator for both the spacecraft attitude matrix and attitude-rate, which mainly uses differential GPS carrier phase measurements, but can also process aiding vector observations (such as low accuracy

coarse Sun sensor measurements, or magnetic field measurements). Conceptually similar to the principle of complementary filtering [7], the idea underlying this estimator is that, due to the different nature of these signals, the combination of both in a unified data processing algorithm can benefit from the relative advantages of both sensor systems, while alleviating the disadvantages of both.

The new estimator is based on a third-order minimal-parameter method for solving the attitude matrix evolution equation using integrated-rate parameters (IRPs) [8]. Similarly to [4, 5], the new estimator is a sequential filtering algorithm and not a deterministic (point estimation) algorithm. However, the new algorithm differs from other works addressing the same problem in two main respects. First, the propagation model of the estimator does not utilize the nonlinear Euler equations. Instead, employing an approach borrowed from linear tracking theory [9], the uncertain dynamic model of the spacecraft is abandoned, and the angular acceleration is modeled as a zero-mean stochastic process with exponential autocorrelation. (A similar, but simpler, approach was employed in the Applied Technology Satellite 6 (ATS-6) [10]). Combined with the extremely simple evolution equation of the IRPs, this results in a simple, linear propagation model. Second, in contrast with other methods relying mainly on the attitude quaternion, the algorithm presented herein directly estimates the attitude matrix, a natural, nonsingular attitude representation. Building upon the minimal, third-order integrated-rate parametrization, the new estimator assigns just three state variables for the parametrization of the nine-parameter attitude matrix, which is at the heart of its computational efficiency.

After a brief review of the IRP method for the solution of the attitude evolution equation, the angular acceleration kinematic model is presented. Applying minimum mean square error (MMSE) estimation theory to the perturbation model, the measurement processing algorithm is developed for both GPS carrier phase signals and vector observations. An attitude matrix orthogonalization procedure, incorporated to enhance the accuracy and robustness of the algorithm, is then introduced, followed by a derivation of the prediction stage. Two numerical examples are then presented, which demonstrate the performance of the new algorithm. Concluding remarks are offered in the last section.

II. INTEGRATED-RATE PARAMETERS

Consider the matrix differential equation

$$\dot{V}(t) = W(t)V(t), \qquad V(t_0) = V_0 \tag{1}$$

where $V(t) \in \mathbb{R}^{n,n}$, $W(t) = -W^T(t)$ for all $t \geq t_0$, $V_0V_0^T = I$ and the overdot indicates the temporal derivative. Defining

$$A(t,t_0) \triangleq \int_{t_0}^{t} W(\tau)d\tau \tag{2}$$

$$\overline{W}_0(t) \triangleq W(t) - (t-t_0)\dot{W}(t) \tag{3}$$

it can be shown [11] that the following matrix-valued function is a third-order approximation of $V(t)$:

$$\tilde{V}(t,t_0) \triangleq \left\{ I + A(t,t_0) + \frac{A^2(t,t_0)}{2!} + \frac{A^3(t,t_0)}{3!} + \frac{t-t_0}{3!} \times [A(t,t_0)\overline{W}_0(t) - \overline{W}_0(t)A(t,t_0)] \right\} V_0. \tag{4}$$

Moreover, $\tilde{V}$ is a third-order approximation of an orthogonal matrix, i.e., $\tilde{V}(t,t_0)\tilde{V}^T(t,t_0) = I + \mathcal{O}((t-t_0)^4)$ where $\mathcal{O}(x)$ denotes a function of x that has the property that $\mathcal{O}(x)/x$ is bounded as $x \to 0$.

In the 3-D case, the off-diagonal entries of $A(t,t_0)$, termed IRPs, have a simple geometric interpretation: they are the angles resulting from a temporal integration of the three components of the angular velocity vector

$$\omega(t) \triangleq [\omega_1(t) \quad \omega_2(t) \quad \omega_3(t)]^T \tag{5}$$

where ω_i is the angular velocity component along the i-axis of the initial coordinate system, and $i = 1,2,3$ for x,y,z, respectively. The orthogonal matrix differential equation (1) is rewritten, in this case, as

$$\dot{D}(t) = \Omega(t)D(t), \qquad D(t_0) = D_0 \tag{6}$$

where $D(t)$ is the attitude matrix, or the direction cosine matrix (DCM), $\Omega(t) = -[\omega(t)\times]$, and $[\omega(t)\times]$ is the *cross product matrix* corresponding to $\omega(t)$, defined as

$$[a\times] \triangleq \begin{bmatrix} 0 & -a_3 & a_2 \\ a_3 & 0 & -a_1 \\ -a_2 & a_1 & 0 \end{bmatrix} \qquad \forall \quad a \in \mathbb{R}^3. \tag{7}$$

(This notation reflects the fact that $[a\times]b = a \times b$ for all $a,b \in \mathbb{R}^3$). In this case, the matrix $A(t,t_0)$ takes the form

$$A(t,t_0) \triangleq -[\theta(t)\times] \tag{8}$$

where the parameter vector $\theta(t)$ is defined as

$$\theta(t) \triangleq [\theta_1(t) \quad \theta_2(t) \quad \theta_3(t)]^T \tag{9}$$

and

$$\theta_i(t) \triangleq \int_{t_0}^{t} \omega_i(\tau)d\tau, \qquad i = 1,2,3. \tag{10}$$

Let the sampling period be denoted by $T \triangleq t_{k+1} - t_k$. Using the notation $\theta(k) \triangleq \theta(t_k)$, the parameter vector at time t_k is $\theta(k) = [\theta_1(k) \; \theta_2(k) \; \theta_3(k)]^T$ and (10)

implies

$$\theta_i(k) = \int_{t_0}^{t_k} \omega_i(\tau)d\tau, \qquad i = 1,2,3. \tag{11}$$

From (11) we have

$$\theta(k+1) = \theta(k) + \int_{t_k}^{t_{k+1}} \omega(\tau)d\tau. \tag{12}$$

Define $A(k+1,k)$ to be the discrete-time analog of $A(t,t_0)$, i.e.,

$$A(k+1,k) \triangleq -[(\theta(k+1) - \theta(k))\times]. \tag{13}$$

Also, let $\Psi(k+1) \triangleq -[\psi(k+1)\times]$, where

$$\psi(k+1) \triangleq \omega(k+1) - \dot{\omega}(k+1)T. \tag{14}$$

Then, the corresponding discrete-time equivalent of (4) is

$$\begin{aligned} D(k+1) = \{&I + A(k+1,k) + \tfrac{1}{2}A^2(k+1,k) \\ &+ \tfrac{1}{6}A^3(k+1,k) + \tfrac{1}{6}T[A(k+1,k)\Psi(k+1) \\ &- \Psi(k+1)A(k+1,k)]\}D(k) \end{aligned} \tag{15}$$

which, using (13) and (14), can be written as

$$D(k+1) = D[\theta(k+1) - \theta(k), \omega(k+1), \dot{\omega}(k+1), D(k)]. \tag{16}$$

III. KINEMATIC MOTION MODEL

To avoid using the uncertain spacecraft dynamic model, the spacecraft angular acceleration is modeled as a zero-mean stochastic process with exponential autocorrelation function. The acceleration dynamic model is, therefore, the following first-order Markov process,

$$\ddot{\omega}(t) = -\Lambda\dot{\omega}(t) + \tilde{\nu}(t). \tag{17}$$

For simplicity, a decoupled kinematic model is chosen for the three angular rate components, i.e., $\Lambda \triangleq \text{diag}\{\tau_1^{-1}, \tau_2^{-1}, \tau_3^{-1}\}$, where $\{\tau_i\}_{i=1}^3$ are the acceleration decorrelation times associated with the corresponding body axes. The driving noise is a zero-mean white process, with power spectral density (PSD) matrix

$$\tilde{Q}(t) = 2\Lambda\Sigma^2, \qquad \Sigma \triangleq \text{diag}\{\sigma_1, \sigma_2, \sigma_3\} \tag{18}$$

The noise variances in (18) were chosen according to the Singer angular acceleration probabilistic model [9], in which the angular acceleration components, $\{\dot{\omega}_i\}_{i=1}^3$, can be 1) equal to $\dot{\omega}_{M_i}$ with probability p_{M_i}, 2) equal to $-\dot{\omega}_{M_i}$ with probability p_{M_i}, 3) equal to zero with probability p_{0_i}, or 4) uniformly distributed over the interval $[-\dot{\omega}_{M_i}, \dot{\omega}_{M_i}]$ with the remaining probability mass. Using this model, it follows that

$$\sigma_i^2 = \frac{\dot{\omega}_{M_i}^2}{3}(1 + 4p_{M_i} - p_{0_i}). \tag{19}$$

The parameters $\dot{\omega}_{M_i}$, p_{M_i}, and p_{0_i} are considered as filter tuning parameters. As customarily done, they are selected by experience with real and simulated data, so as to optimally adapt the filter to the characteristics of the problem at hand.

Defining now the state vector of the system as

$$x(t) \triangleq [\theta^T(t) \quad \omega^T(t) \quad \dot{\omega}^T(t)]^T \tag{20}$$

the state equation is

$$\dot{x}(t) = Fx(t) + \tilde{\nu}(t) \equiv \begin{bmatrix} 0 & I & 0 \\ 0 & 0 & I \\ 0 & 0 & -\Lambda \end{bmatrix} x(t) + \begin{bmatrix} 0 \\ 0 \\ \tilde{\nu}(t) \end{bmatrix} \tag{21}$$

with obvious definitions of F and $\tilde{\nu}(t)$. Corresponding to the sampling interval T, the discrete-time state equation is

$$x(k+1) = \Phi(T)x(k) + \nu(k) \tag{22}$$

where the transition matrix is

$$\Phi(T) \equiv e^{FT} = \begin{bmatrix} I & TI & \Lambda^{-2}(e^{-\Lambda T} - I + T\Lambda) \\ 0 & I & \Lambda^{-1}(I - e^{-\Lambda T}) \\ 0 & 0 & e^{-\Lambda T} \end{bmatrix} \tag{23}$$

and $\nu(k)$ is a zero-mean, white noise sequence, with covariance matrix

$$\begin{aligned} Q(k) &\triangleq E\{\nu(k)\nu^T(k)\} \\ &= \int_0^T e^{F(T-t)}\text{diag}\{0,0,\tilde{Q}(t)\}e^{F^T(T-t)}dt. \end{aligned} \tag{24}$$

Explicit computation of the integrals in (24) yields the following expressions for the entries of the symmetric covariance matrix $Q(k)$

$$\begin{aligned} Q_{11}(k) = \Lambda^{-4}\Sigma^2(&I + 2\Lambda T - 2\Lambda^2T^2 + \tfrac{2}{3}\Lambda^3T^3 \\ &- e^{-2\Lambda T} - 4\Lambda T e^{-\Lambda T}) \end{aligned} \tag{25a}$$

$$\begin{aligned} Q_{12}(k) = \Lambda^{-3}\Sigma^2(&I - 2\Lambda T + \Lambda^2T^2 - 2e^{-\Lambda T} \\ &+ e^{-2\Lambda T} + 2\Lambda T e^{-\Lambda T}) \end{aligned} \tag{25b}$$

$$Q_{13}(k) = \Lambda^{-2}\Sigma^2(I - e^{-2\Lambda T} - 2\Lambda T e^{-\Lambda T}) \tag{25c}$$

$$Q_{22}(k) = \Lambda^{-2}\Sigma^2(4e^{-\Lambda T} - 3I - e^{-2\Lambda T} + 2\Lambda T) \tag{25d}$$

$$Q_{23}(k) = \Lambda^{-1}\Sigma^2(e^{-2\Lambda T} + I - 2e^{-\Lambda T}) \tag{25e}$$

$$Q_{33}(k) = \Sigma^2(I - e^{-2\Lambda T}). \tag{25f}$$

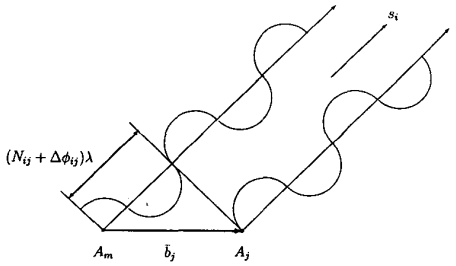

Fig. 1. GPS phase difference measurement geometry.

IV. MEASUREMENT PROCESSING

A. GPS Differential Phase Measurements

Consider the basic GPS antenna array, depicted in Fig. 1. The array consists of the master antenna A_m and the slave antenna A_j. These antennae are located on the surface of the satellite, such that the baseline vector between them, resolved in a body-fixed coordinate system, is $\bar{b}_j$. It is assumed that the entire system consists of m_b antennae, in addition to the master antenna, so that there exist m_b independent baselines. It is also assumed that at time t_{k+1}, m_s GPS satellites are in view.

Consider the ith satellite, and denote the sightline (unit) direction vector to that satellite, resolved in an inertial coordinate system, by s_i. Let $D(k+1)$ be the attitude matrix transforming vectors in the inertial coordinate system to their body-fixed system representations at time t_{k+1}. Let $N_{ij}(k+1)$ and $\Delta\phi_{ij}(k+1)$ denote the integer and fractional parts, respectively, of the phase difference between the two carrier signals, corresponding to the ith satellite, as acquired by the antennae A_m and A_j. Denoting by Λ the GPS carrier wavelength, the true (noiseless) signals satisfy

$$[\Delta\phi_{ij}(k+1) + N_{ij}(k+1)]\lambda = \bar{b}_j^T D(k+1)s_i. \quad (26)$$

The standard GPS carrier wavelength is 19.03 cm. In this work, it is assumed that the integer part of the phase difference between the two receivers is known from a previous solution [1, 12].

In practice, the phase measurements are contaminated by noise, the primary source of which is due to the multipath effect [1]. Denoting the noise corresponding to the baseline $\bar{b}_j$ and the sightline s_i by $\tilde{n}_{ij}(k+1)$, the real measurement equation is

$$[\Delta\phi_{ij}(k+1) + N_{ij}(k+1)]\lambda = \bar{b}_j^T D(k+1)s_i + \tilde{n}_{ij}(k+1) \quad (27)$$

where it is assumed that $\tilde{n}_{ij}(k+1) \sim \mathcal{N}(0, \tilde{\sigma}_{ij}^2(k+1))$. Typically it can be assumed that the noise standard deviation is on the order of 5 mm [1]. From (27) we obtain the normalized measurement equation

$$\Delta\phi_{ij}(k+1) + N_{ij}(k+1) = b_j^T D(k+1)s_i + n_{ij}(k+1) \quad (28)$$

where we have defined $b_j \triangleq \bar{b}_j/\lambda$ and $n_{ij}(k+1) \triangleq \tilde{n}_{ij}(k+1)/\lambda$. The normalized measurement noise satisfies $n_{ij}(k+1) \sim \mathcal{N}(0, \sigma_{ij}^2(k+1))$, where

$$\sigma_{ij}(k+1) = \tilde{\sigma}_{ij}(k+1)/\lambda. \quad (29)$$

1) *GPS Measurement Linearization*: At t_{k+1} the MMSE predicted vector is $\hat{x}(k+1 \mid k)$, and its corresponding prediction error covariance matrix is $P(k+1 \mid k) \triangleq E\{\tilde{x}(k+1 \mid k)\tilde{x}^T(k+1 \mid k)\}$, where the estimation error is

$$\tilde{x}(j \mid k) \triangleq x(j) - \hat{x}(j \mid k). \quad (30)$$

Using (16), (28) is rewritten as

$$\begin{aligned} N_{ij}(k+1) &+ \Delta\phi_{ij}(k+1) \\ &= b_j^T D[\theta(k+1) - \theta(k), \omega(k+1), \dot{\omega}(k+1), D(k)]s_i \\ &\quad + n_{ij}(k+1). \end{aligned} \quad (31)$$

Next, we linearize the nonlinear measurement equation (31) about the most recent estimate at t_{k+1}, i.e.,

$$\begin{aligned} x(k+1) &= \hat{x}(k+1 \mid k) + \delta x(k+1) \\ &\equiv \begin{bmatrix} \hat{\theta}(k+1 \mid k) \\ \hat{\omega}(k+1 \mid k) \\ \hat{\dot{\omega}}(k+1 \mid k) \end{bmatrix} + \begin{bmatrix} \delta\theta(k+1) \\ \delta\omega(k+1) \\ \delta\dot{\omega}(k+1) \end{bmatrix} \end{aligned} \quad (32)$$

where $\delta\theta(k+1)$, $\delta\omega(k+1)$, and $\delta\dot{\omega}(k+1)$ are the perturbations of the state components about the nominal (i.e., predicted) state. Let $\hat{D}^*(k \mid k)$ denote the a posteriori, *orthogonalized* estimate of the attitude matrix at time t_k, to be discussed in the next section. Using now the most recent estimates for $D(k)$ and $x(k)$, namely $\hat{D}^*(k \mid k)$ and $\hat{x}(k \mid k)$, respectively, in (31), it follows that

$$\begin{aligned} \Delta\phi_{ij}(k+1) &+ N_{ij}(k+1) \\ &= b_j^T D[\hat{\theta}(k+1 \mid k) + \delta\theta(k+1) - \hat{\theta}(k \mid k), \\ &\qquad \hat{\omega}(k+1 \mid k) + \delta\omega(k+1), \\ &\qquad \hat{\dot{\omega}}(k+1 \mid k) + \delta\dot{\omega}(k+1), \hat{D}^*(k \mid k)]s_i + n_{ij}(k+1). \end{aligned} \quad (33)$$

As discussed in the sequel, the a posteriori IRP estimate is zeroed after each measurement update (due to full reset control of the IRP state). We, therefore, use the reset value of the IRP estimate, $\hat{\theta}^c(k \mid k) = 0$, in (33). Now expand D about the nominal state using a first-order Taylor series expansion, i.e.,

$$
\begin{aligned}
&D[\hat{\theta}(k+1\mid k)+\delta\theta(k+1),\hat{\omega}(k+1\mid k)+\delta\omega(k+1),\hat{\dot{\omega}}(k+1\mid k)+\delta\dot{\omega}(k+1),\hat{D}^*(k\mid k)]\\
&\quad=\hat{D}(k+1\mid k)+\sum_{i=1}^{3}\left.\frac{\partial D[\theta(k+1),\hat{\omega}(k+1\mid k),\hat{\dot{\omega}}(k+1\mid k),\hat{D}^*(k\mid k)]}{\partial\theta_i}\right|_{\hat{\theta}(k+1|k)}\delta\theta_i(k+1)\\
&\quad\quad+\sum_{i=1}^{3}\left.\frac{\partial D[\hat{\theta}(k+1\mid k),\omega(k+1),\hat{\dot{\omega}}(k+1\mid k),\hat{D}^*(k\mid k)]}{\partial\omega_i}\right|_{\hat{\omega}(k+1|k)}\delta\omega_i(k+1)\\
&\quad\quad+\sum_{i=1}^{3}\left.\frac{\partial D[\hat{\theta}(k+1\mid k),\hat{\omega}(k+1\mid k),\dot{\omega}(k+1),\hat{D}^*(k\mid k)]}{\partial\dot{\omega}_i}\right|_{\hat{\omega}(k+1|k)}\delta\dot{\omega}_i(k+1)
\end{aligned}
\tag{34}
$$

where $(\bullet)|_\zeta$ denotes "evaluated at ζ" and

$$
\hat{D}(k+1\mid k)\triangleq D[\hat{\theta}(k+1\mid k),\hat{\omega}(k+1\mid k),\hat{\dot{\omega}}(k+1\mid k),\hat{D}^*(k\mid k)]. \tag{35}
$$

Differentiating (15), the sensitivity matrices appearing in (34) are computed as

$$
\begin{aligned}
&\frac{\partial}{\partial\theta_i}D[\theta(k+1),\hat{\omega}(k+1\mid k),\hat{\dot{\omega}}(k+1\mid k),\hat{D}^*(k\mid k)]\\
&\quad=G_i[\theta(k+1),\hat{\psi}(k+1\mid k)]\hat{D}^*(k\mid k) &\text{(36a)}\\
&\frac{\partial}{\partial\omega_i}D[\hat{\theta}(k+1\mid k),\omega(k+1),\hat{\dot{\omega}}(k+1\mid k),\hat{D}^*(k\mid k)]\\
&\quad=\tfrac{1}{6}TF_i[\hat{\theta}(k+1\mid k)]\hat{D}^*(k\mid k) &\text{(36b)}\\
&\frac{\partial}{\partial\dot{\omega}_i}D[\hat{\theta}(k+1\mid k),\hat{\omega}(k+1\mid k),\dot{\omega}(k+1),\hat{D}^*(k\mid k)]\\
&\quad=-\tfrac{1}{6}T^2F_i[\hat{\theta}(k+1\mid k)]\hat{D}^*(k\mid k) &\text{(36c)}
\end{aligned}
$$

for $i=1,2,3$, where

$$
\hat{\psi}(k+1\mid k)\triangleq\hat{\omega}(k+1\mid k)-T\hat{\dot{\omega}}(k+1\mid k) \tag{37}
$$

and

$$
\begin{aligned}
G_i(\theta,\psi)&=\tfrac{1}{2}(\theta e_i^T+e_i\theta^T)-\theta_i I-(1-\tfrac{1}{6}\|\theta\|^2)[e_i\times]\\
&\quad+\tfrac{1}{6}T(\psi e_i^T-e_i\psi^T)+\tfrac{1}{3}\theta_i[\theta\times] &\text{(38a)}\\
F_i(\theta)&=e_i\theta^T-\theta e_i^T &\text{(38b)}
\end{aligned}
$$

where e_i is the unit vector on the ith axis, $i=1,2,3$.

Using (34), (36), and (38) in (33) yields

$$
\begin{aligned}
&\Delta\phi_{ij}(k+1)+N_{ij}(k+1)-b_j^T\hat{D}(k+1\mid k)s_i\\
&\quad=h_{ij}^T(k+1)\delta x(k+1)+n_{ij}(k+1)
\end{aligned}
\tag{39}
$$

where the observation vector $h_{ij}(k+1)\in\mathbb{R}^9$ is defined as

$$
h_{ij}(k+1)\equiv[h_{\theta_{ij}}^T(k+1)\quad h_{\omega_{ij}}^T(k+1)\quad h_{\dot{\omega}_{ij}}^T(k+1)]^T \tag{40}
$$

and the elements of the vectors $h_{\theta_{ij}}(k+1)\in\mathbb{R}^3$, $h_{\omega_{ij}}(k+1)\in\mathbb{R}^3$ and $h_{\dot{\omega}_{ij}}(k+1)\in\mathbb{R}^3$ are

$$
h_{\theta_{ijp}}(k+1)=b_j^TG_p[\hat{\theta}(k+1\mid k),\hat{\psi}(k+1\mid k)]\hat{D}^*(k\mid k)s_i,\quad p=1,2,3 \tag{41a}
$$

$$
h_{\omega_{ijp}}(k+1)=\tfrac{1}{6}Tb_j^TF_p[\hat{\theta}(k+1\mid k)]\hat{D}^*(k\mid k)s_i,\quad p=1,2,3 \tag{41b}
$$

$$
h_{\dot{\omega}_{ijp}}(k+1)=-Th_{\omega_{ijp}}(k+1),\quad p=1,2,3 \tag{41c}
$$

Define now the *effective* GPS measurement to be

$$
y_{ij}^\phi(k+1)\triangleq\Delta\phi_{ij}(k+1)+N_{ij}-b_j^T\hat{D}(k+1\mid k)s_i. \tag{42}
$$

Then, using this definition in (39) yields the following scalar measurement equation:

$$
y_{ij}^\phi(k+1)=h_{ij}^T(k+1)\delta x(k+1)+n_{ij}(k+1). \tag{43}
$$

For the m_b baselines and m_s sightlines, there exist $m_s\times m_b$ scalar measurements like (43). We next aggregate all of these equations into a single vector equation, such that the measurement associated with the baseline b_j and sightline s_i corresponds to the pth component of the vector measurement equation, where $p=(j-1)m_s+i$. This yields

$$
y^\phi(k+1)=H^\phi(k+1)\delta x(k+1)+n^\phi(k+1) \tag{44}
$$

where the pth row of the matrix $H^\phi(k+1)$ is $h_{ij}^T(k+1)$, the measurement noise satisfies

$$
n^\phi(k+1)\sim\mathcal{N}(0,R^\phi(k+1)) \tag{45}
$$

and the covariance $R^\phi(k+1)$ is a diagonal matrix whose diagonal elements are

$$
R_{pp}^\phi(k+1)=\sigma_{ij}^2. \tag{46}
$$

B. Vector Observation Aiding

If the sole source of attitude information is the GPS carrier phase signals, then (44) should serve as the basis for the development of the measurement update algorithm (in the next section). In the case that vector observations are available, this information structure needs to be augmented.

Assume that a new pair of corresponding noisy vector measurements is acquired at t_{k+1}. This pair consists of the *unit* vectors $u(k+1)$ and $v(k+1)$, which represent the values of the same vector $r(k+1)$, as modeled in the reference coordinate system and measured in the body coordinate system, respectively. The DCM $D(k+1)$ transforms the *true* vector representation u_0 into its corresponding *true* representation v_0 according to

$$v_0(k+1) = D(k+1)u_0(k+1). \tag{47}$$

Assuming no constraint on the measurement noise direction, the body-frame measured unit vector $v(k+1)$ is related to the true vector according to

$$v(k+1) = \frac{v_0(k+1) + n_v'(k+1)}{\|v_0(k+1) + n_v'(k+1)\|} \tag{48}$$

where the white sensor measurement noise is $n_v'(k+1) \sim \mathcal{N}(0, R_v'(k+1))$. Since both $v_0(k+1)$ and $v(k+1)$ are unit vectors, it follows from (48) that

$$v(k+1) = v_0(k+1) + n_v(k+1) \tag{49}$$

where $n_v(k+1) \triangleq \mathcal{P}_{v_0}^{\perp}(k+1)n_v'(k+1)$ and $\mathcal{P}_{v_0}^{\perp}(k+1) \triangleq I - v_0(k+1)v_0^T(k+1)$ is the orthogonal projector onto the orthogonal complement of span$\{v_0(k+1)\}$. To a good approximation, the effective measurement noise is a zero-mean, white Gaussian sequence with covariance

$$R_v(k+1) = \mathcal{P}_{v_0}^{\perp}(k+1)R_v'(k+1)\mathcal{P}_{v_0}^{\perp}(k+1). \tag{50}$$

To account for nonideal effects (e.g., star catalog errors), it is assumed that the modeled reference vector is related to the true vector according to

$$u(k+1) = u_0(k+1) + n_u(k+1) \tag{51}$$

where $n_u \perp u_0$ is a zero mean, white Gaussian noise, that is uncorrelated with n_v and has a known covariance matrix $R_u(k)$.

1) *Vector Measurement Linearization*: Using (16), (47) can be rewritten as

$$v_0(k+1) = D[\theta(k+1) - \theta(k), \omega(k+1), \dot{\omega}(k+1), D(k)]u_0(k+1). \tag{52}$$

Linearizing about the predicted estimates and using (32), (49), and (51), it follows that

$$\begin{aligned} v(k+1) - n_v(k+1) &= D[\hat{\theta}(k+1 \mid k) + \delta\theta(k+1), \hat{\omega}(k+1 \mid k) + \delta\omega(k+1), \\ &\quad \hat{\dot{\omega}}(k+1 \mid k) + \delta\dot{\omega}(k+1), \hat{D}^*(k \mid k)] \\ &\quad \times [u(k+1) - n_u(k+1)] \end{aligned} \tag{53}$$

where, as previously done in the GPS measurement linearization, the reset value of the IRP estimate, $\hat{\theta}^c(k \mid k) = 0$, has been used. Expanding D about the nominal state using the first-order Taylor series (34) yields

$$\begin{aligned} &v(k+1) - \hat{D}(k+1 \mid k)u(k+1) \\ &= \sum_{i=1}^{3} [G_i[\hat{\theta}(k+1 \mid k), \hat{\psi}(k+1 \mid k)]\delta\theta_i(k+1) \\ &\quad + \tfrac{1}{6}TF_i[\hat{\theta}(k+1 \mid k)]\delta\omega_i(k+1) \\ &\quad - \tfrac{1}{6}T^2F_i[\hat{\theta}(k+1 \mid k)]\delta\dot{\omega}_i(k+1)]\hat{D}^*(k \mid k)u(k+1) \\ &\quad - \hat{D}(k+1 \mid k)n_u(k+1) + n_v(k+1) \\ &= H^v(k+1)\delta x(k+1) - \hat{D}(k+1 \mid k)n_u(k+1) + n_v(k+1) \end{aligned} \tag{54}$$

where the observation matrix $H^v(k+1)$ is written in block matrix form as

$$H^v(k+1) \equiv [H_1(k+1) \quad H_2(k+1) \quad H_3(k+1)] \tag{55}$$

and the columns of the submatrices $H_i(k+1) \in \mathbb{R}^{3,3}$, $i = 1,2,3$ are

$$H_{1_j}(k+1) = G_j[\hat{\theta}(k+1 \mid k), \hat{\psi}(k+1 \mid k)] \times \hat{D}^*(k \mid k)u(k+1) \tag{56a}$$

$$H_{2_j}(k+1) = \tfrac{1}{6}TF_j[\hat{\theta}(k+1 \mid k)]\hat{D}^*(k \mid k)u(k+1) \tag{56b}$$

$$H_{3_j}(k+1) = -TH_{2_j}(k+1) \tag{56c}$$

for $j = 1,2,3$. Notice that the same sensitivity matrices are used here, as in the linearized GPS measurement equation, which implies obvious computational saving. Define now the *effective* measurement and measurement noise to be, respectively,

$$y^v(k+1) \triangleq v(k+1) - \hat{D}(k+1 \mid k)u(k+1) \tag{57}$$

$$n^v(k+1) \triangleq n_v(k+1) - \hat{D}(k+1 \mid k)n_u(k+1). \tag{58}$$

Then, using these definitions in (54) yields the following measurement equation:

$$y^v(k+1) = H^v(k+1)\delta x(k+1) + n^v(k+1) \tag{59}$$

where $n^{\nu}(k+1) \sim \mathcal{N}(0, R^{\nu}(k+1))$ is the white measurement noise, and

$$R^{\nu}(k+1) \triangleq R_{v}(k+1) + \hat{D}(k+1 \mid k) R_{u}(k+1) \hat{D}^{T}(k+1 \mid k). \tag{60}$$

C. Measurement Update

To process the measurements, define now

$$y \triangleq \begin{bmatrix} y^{\phi} \\ y^{\nu} \end{bmatrix}, \qquad H \triangleq \begin{bmatrix} H^{\phi} \\ H^{\nu} \end{bmatrix}, \qquad n \triangleq \begin{bmatrix} n^{\phi} \\ n^{\nu} \end{bmatrix} \tag{61}$$

where $n \sim \mathcal{N}(0, R)$ and $R \triangleq \operatorname{diag}\{R^{\phi}, R^{\nu}\}$. Since

$$\delta x(k+1) = x(k+1) - \hat{x}(k+1 \mid k) = \tilde{x}(k+1 \mid k) \tag{62}$$

and $\hat{x}(k+1 \mid k)$ is an unbiased MMSE predictor, we have

$$E\{\delta x(k+1)\} = E\{\tilde{x}(k+1 \mid k)\} = 0 \tag{63}$$

and

$$\operatorname{cov}\{\delta x(k+1)\} = \operatorname{cov}\{\tilde{x}(k+1 \mid k)\} = P(k+1 \mid k) \tag{64}$$

thus

$$\delta x(k+1) \sim \mathcal{N}(0, P(k+1 \mid k)). \tag{65}$$

Using the linearized measurement equation and the statistical properties of the measurement and prediction errors, the MMSE estimator of $\delta x(k+1)$ is

$$\widehat{\delta x}(k+1 \mid k+1) = K(k+1) y(k+1) \tag{66}$$

where $K(k+1)$, the estimator gain matrix, is computed as

$$K(k+1) = P(k+1 \mid k) H^{T}(k+1) \times [H(k+1) P(k+1 \mid k) H^{T}(k+1) + R(k+1)]^{-1}. \tag{67}$$

Also, $\widehat{\delta x}(k+1 \mid k+1) = \hat{x}(k+1 \mid k+1) - \hat{x}(k+1 \mid k)$ which, used in (66), yields the state measurement update equation

$$\hat{x}(k+1 \mid k+1) = \hat{x}(k+1 \mid k) + K(k+1) y(k+1). \tag{68}$$

Subtracting $x(k+1)$ from both sides of the last equation yields

$$\tilde{x}(k+1 \mid k+1) = [I - K(k+1) H(k+1)] \tilde{x}(k+1 \mid k) - K(k+1) n(k+1) \tag{69}$$

from which the resulting covariance update equation is

$$P(k+1 \mid k+1) = [I - K(k+1) H(k+1)] P(k+1 \mid k) \times [I - K(k+1) H(k+1)]^{T} + K(k+1) R(k+1) K^{T}(k+1) \tag{70}$$

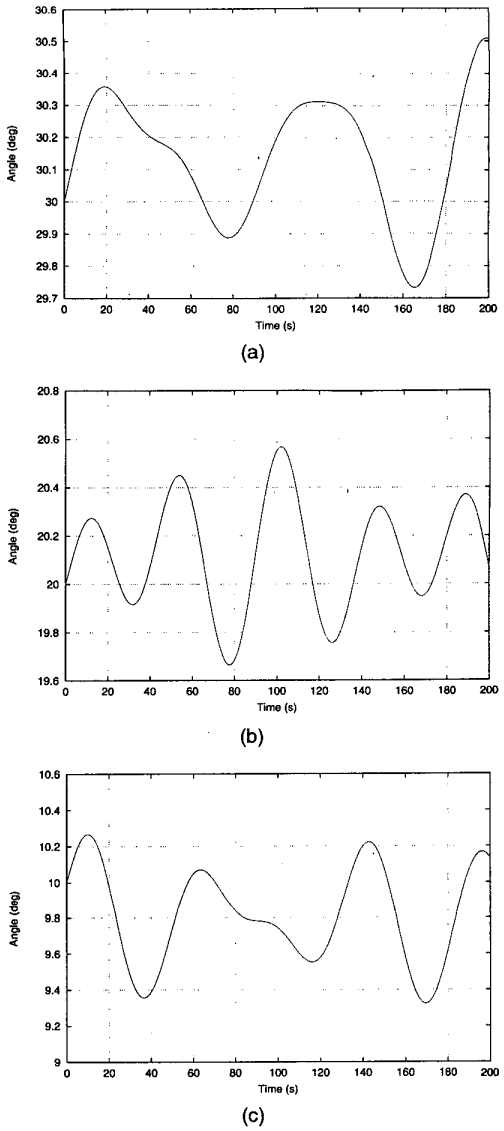

Fig. 2. Example I. True Euler angles. (a) Roll angle. (b) Pitch angle. (c) Yaw angle.

where the filtering error covariance is $P(k+1 \mid k+1) \triangleq E\{\tilde{x}(k+1 \mid k+1) \tilde{x}^{T}(k+1 \mid k+1)\}$.

To compute the measurement-updated attitude matrix at time t_{k+1}, we use the most recent estimate $\hat{x}(k+1 \mid k+1)$ and the estimated attitude matrix corresponding to time t_k in (15). This yields

$$\hat{D}(k+1 \mid k+1) = \{I + \hat{A}(k+1,k) + \tfrac{1}{2}\hat{A}^{2}(k+1,k) + \tfrac{1}{6}\hat{A}^{3}(k+1,k) + \tfrac{1}{6}T[\hat{A}(k+1,k)\hat{\Psi}(k+1 \mid k+1) - \hat{\Psi}(k+1 \mid k+1)\hat{A}(k+1,k)]\}\hat{D}^{*}(k \mid k) \tag{71}$$

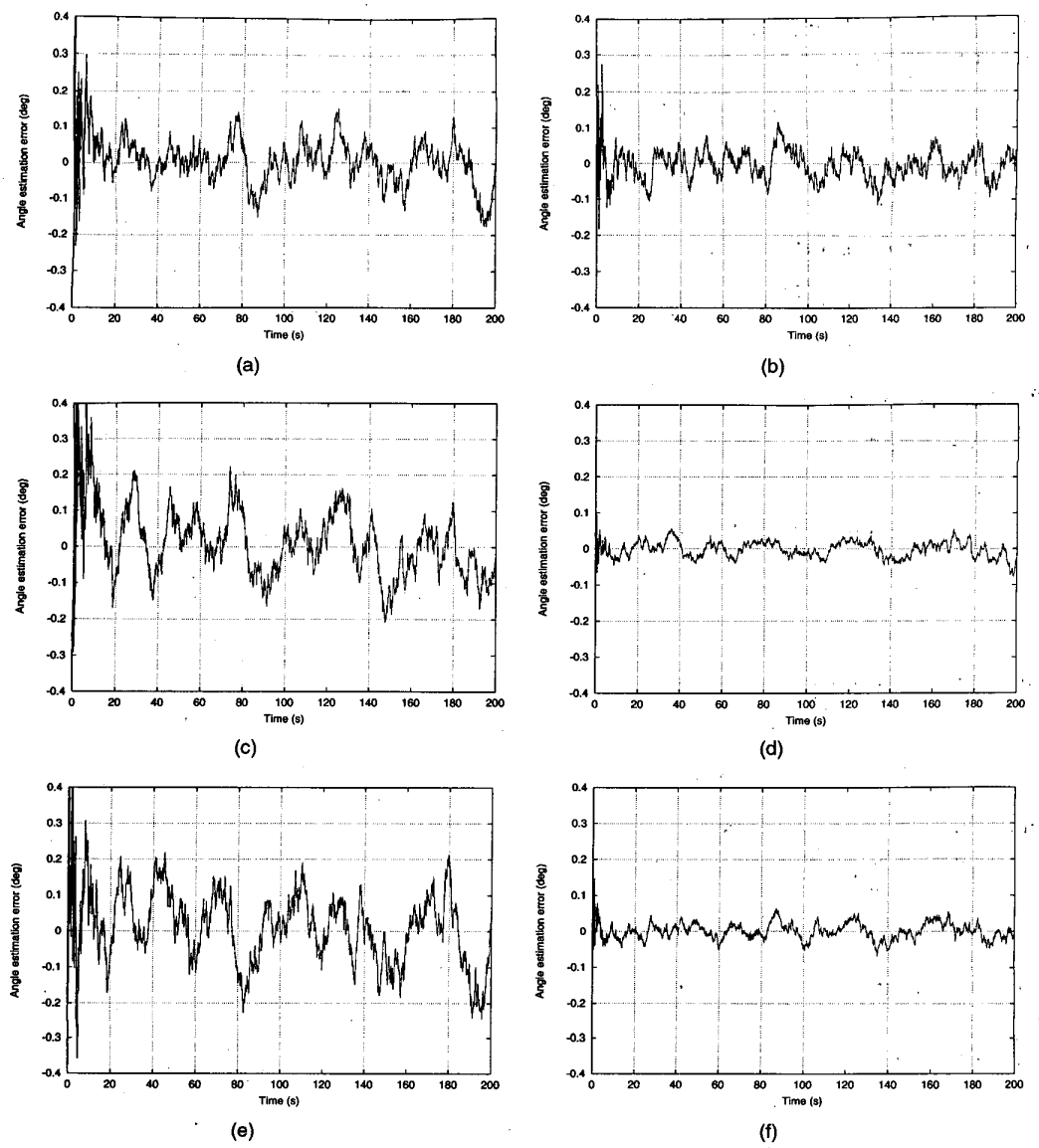

Fig. 3. Example I. Effect of vector observation aiding on Euler angle estimation. (a) Roll, GPS only. (b) Roll, with vector observation aiding. (c) Pitch, GPS only. (d) Pitch, with vector observation aiding. (e) Yaw, GPS only. (f) Yaw, with vector observation aiding.

where the *a posteriori* estimates of $A(k+1,k)$ and $\Psi(k+1)$ are defined, respectively, as

$$\hat{A}(k+1,k) \triangleq -[\hat{\theta}(k+1 \mid k+1)\times] \tag{72}$$

$$\hat{\Psi}(k+1 \mid k+1) \triangleq -[\hat{\psi}(k+1 \mid k+1)\times] \tag{73}$$

where

$$\hat{\psi}(k+1 \mid k+1) \triangleq \hat{\omega}(k+1 \mid k+1) - T\hat{\dot{\omega}}(k+1 \mid k+1) \tag{74}$$

and $\hat{D}^{*}(k \mid k)$ is the a posteriori, *orthogonalized* estimate of the attitude matrix at time t_k, to be discussed in the next section.

Finally, since the a posteriori attitude matrix $\hat{D}(k+1 \mid k+1)$ is computed based on the a posteriori estimate $\hat{\theta}(k+1 \mid k+1)$, this implies a full *reset control* [13, p. 332] of the parameter vector, i.e.,

$$\theta^{c}(k+1) = \theta(k+1) - \hat{\theta}(k+1 \mid k+1) \tag{75}$$

where $\theta^{c}(k+1)$ is the *reset* state vector at t_{k+1}, and a corresponding reset of the state estimate,

$$\hat{\theta}^{c}(k+1 \mid k+1) = 0 \tag{76}$$

which is then used in the ensuing time propagation step. Since the reset control is applied to *both* the state vector and its estimate, no changes are necessary in the estimation error covariance matrix.

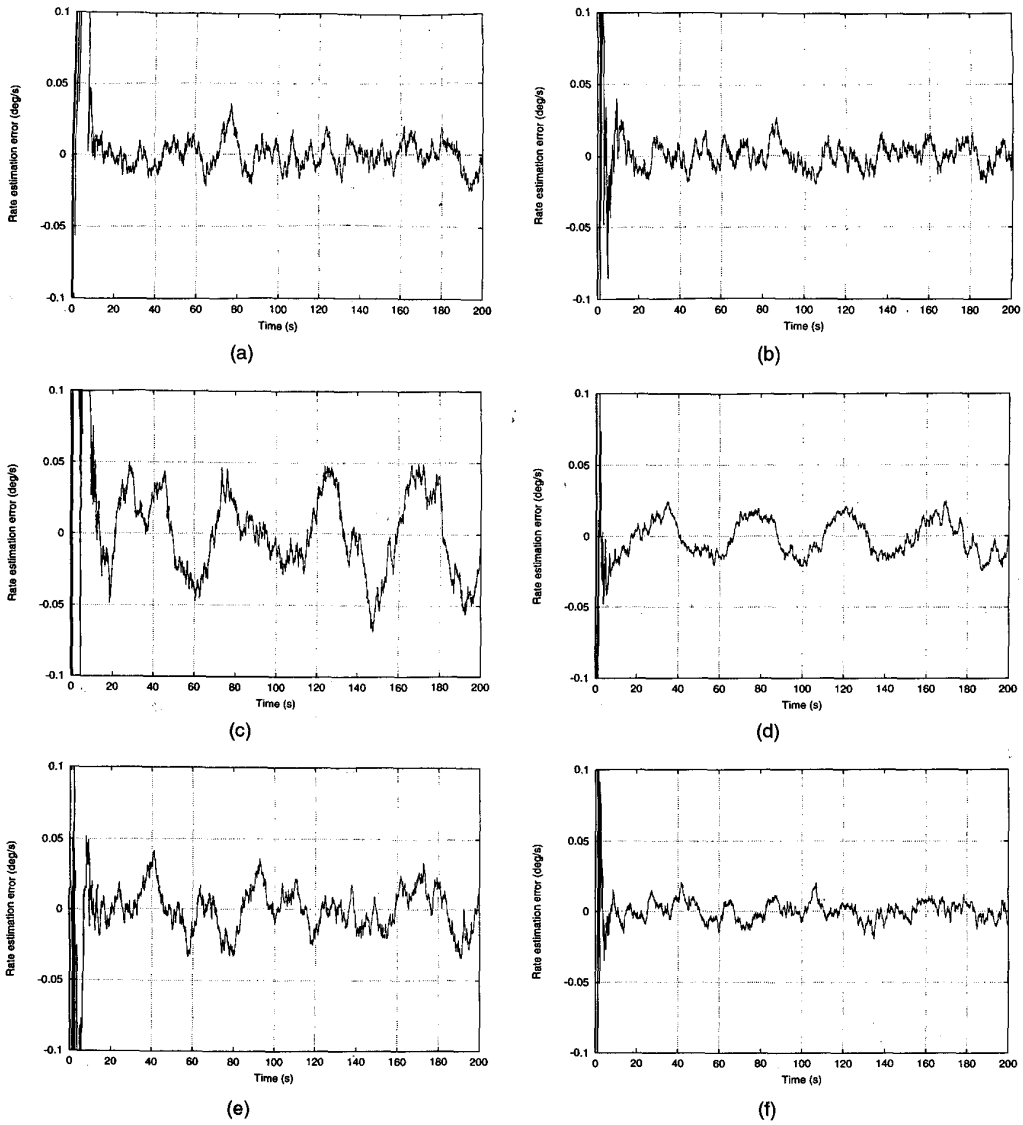

Fig. 4. Example I. Effect of vector observation aiding on angular rate estimation. (a) ω_1, GPS only. (b) ω_1, with vector observation aiding. (c) ω_2, GPS only. (d) ω_2, with vector observation aiding. (e) ω_3, GPS only. (f) ω_3, with vector observation aiding.

V. ATTITUDE MATRIX ORTHOGONALIZATION

To improve the accuracy of the algorithm, and enhance its stability, an additional orthogonalization procedure is introduced into the estimator, following the measurement update stage. In this procedure, the attitude matrix closest to the filtered attitude matrix is computed.

Given the filtered attitude matrix $\hat{D}(k+1 \mid k+1)$, the attitude matrix orthogonalization problem is to find the matrix

$$\hat{D}^*(k+1 \mid k+1) \triangleq \arg \min_{D \in \mathbb{R}^{3,3}} \|\hat{D}(k+1 \mid k+1) - D\| \tag{77a}$$

subject to

$$D^T D = I \quad \text{and} \quad \det D = +1. \tag{77b}$$

Being a special case of the orthogonal Procrustes problem [14], the matrix orthogonalization problem can be easily solved using the singular value decomposition (SVD) [15]. Thus, if

$$\hat{D}(k+1 \mid k+1) = U(k+1)\Sigma(k+1)V^T(k+1) \tag{78}$$

is the SVD of the matrix $\hat{D}(k+1 \mid k+1)$ where $U(k+1)$ and $V(k+1)$ are the left and right singular vector matrices, respectively, and $\Sigma(k+1) = \text{diag}\{s_1, s_2, s_3\}$ is the singular value matrix where

$s_1 \geq s_2 \geq s_3$, then

$$\hat{D}^*(k+1 \mid k+1) = U(k+1)\text{diag}\{1,1,\det U(k+1)\det V(k+1)\}V^T(k+1). \tag{79}$$

In real-time attitude determination and control the excessive computational burden associated with the SVD might render its use prohibitive. In such cases, the following approximate orthogonalization method, consisting of a single-step application of the iterative method introduced in [16], can be utilized

$$\hat{D}^*(k+1 \mid k+1) = N(k+1)\hat{D}(k+1 \mid k+1) \tag{80}$$

where

$$N(k+1) \triangleq \tfrac{3}{2}I - \tfrac{1}{2}\hat{D}(k+1 \mid k+1)\hat{D}^T(k+1 \mid k+1). \tag{81}$$

REMARK 1 Using an approach similar to that used in [17], it can be shown that, to first-order, the orthogonalization procedure does not affect the statistical properties of the estimator and, therefore, does not necessitate any adjustments in the algorithm.

VI. PREDICTION

In the prediction step at t_k, the reset a posteriori estimate at time t_k, $\hat{x}^c(k \mid k)$ (computed with the reset IRP estimate) and its corresponding error covariance matrix $P(k \mid k)$, are propagated to time t_{k+1}.

Using (22), we have

$$\hat{x}(k+1 \mid k) = \Phi(T)\hat{x}^c(k \mid k). \tag{82}$$

Using this result with (22) yields the covariance propagation equation

$$P(k+1 \mid k) = \Phi(T)P(k \mid k)\Phi^T(T) + \Gamma(T)Q(k)\Gamma^T(T). \tag{83}$$

To propagate the attitude matrix to t_{k+1} we use the most recent IRP, attitude-rate and angular acceleration estimates, and the orthogonalized DCM estimate corresponding to t_k, in (15). This yields

$$\begin{aligned}\hat{D}(k+1 \mid k) = \{&I + \overline{A}(k+1,k) + \tfrac{1}{2}\overline{A}^2(k+1,k) \\ &+ \tfrac{1}{6}\overline{A}^3(k+1,k) \\ &+ \tfrac{1}{6}T[\overline{A}(k+1,k)\hat{\Psi}(k+1 \mid k) \\ &- \hat{\Psi}(k+1 \mid k)\overline{A}(k+1,k)]\}\hat{D}^*(k \mid k)\end{aligned} \tag{84}$$

where the *a priori* estimates of $A(k+1,k)$ and $\Psi(k+1)$ are defined, respectively, as

$$\overline{A}(k+1,k) \triangleq -[\hat{\theta}(k+1 \mid k)\times] \tag{85}$$

$$\hat{\Psi}(k+1 \mid k) \triangleq -[\hat{\dot{\psi}}(k+1 \mid k)\times]. \tag{86}$$

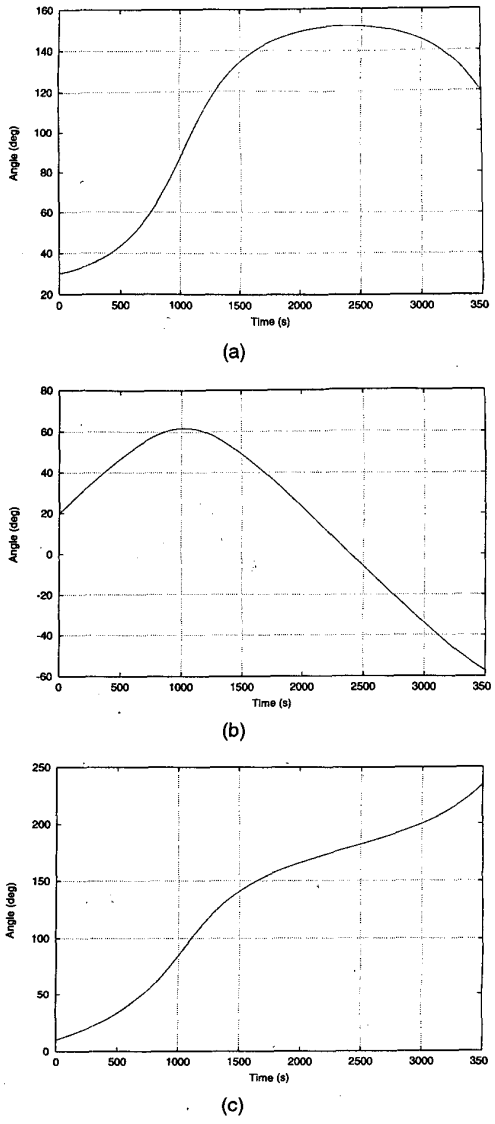

Fig. 5. Example II: True Euler angles. (a) Roll angle. (b) Pitch angle. (c) Yaw angle.

VII. NUMERICAL STUDY

Two numerical examples are presented in this section, to demonstrate the performance of the new estimator, and illustrate the performance enhancement achieved by using aiding vector observations.

A. Example I

In this example, three nonorthogonal baselines were used: $\overline{b}_1 = [1.0, 1.0, 0.0]^T$, $\overline{b}_2 = [0.0,\ 1.0, 0.0]^T$, $\overline{b}_3 = [0.0, 0.0, 1.0]^T$. Two fixed sightlines were observed at all times, $s_1 = 1/\sqrt{3}[1.0, 1.0, 1.0]^T$ and $s_2 = 1/\sqrt{2}[0.0, 1.0, 1.0]^T$. The nonnormalized GPS signal noise standard deviation was 5.0 mm. When vector measurements were used, the noise equivalent angle of the inertially referenced observations was

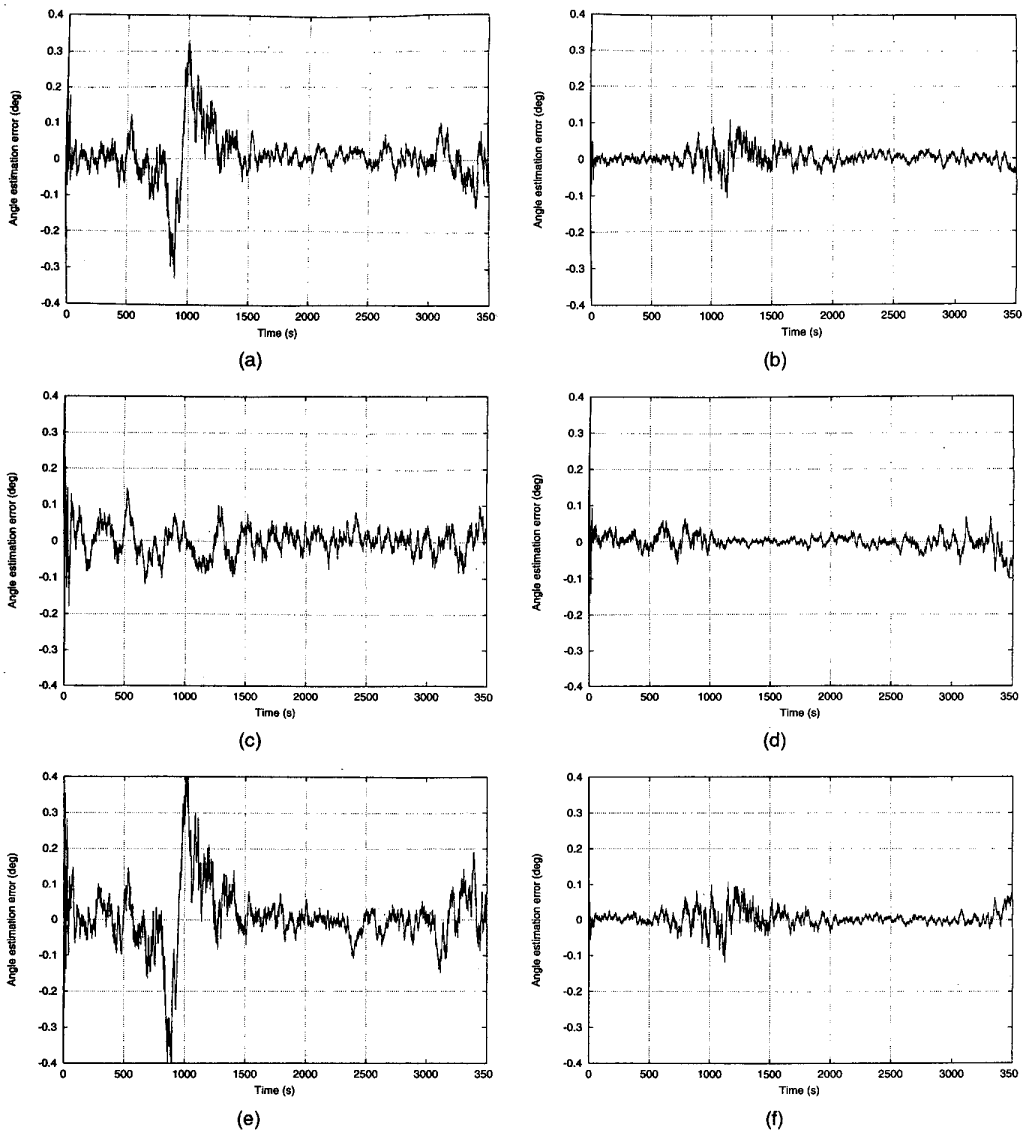

Fig. 6. Example II: Effect of vector observation aiding on Euler angle estimation. (a) Roll, GPS only. (b) Roll, with vector observation aiding. (c) Pitch, GPS only. (d) Pitch, with vector observation aiding. (e) Yaw, GPS only. (f) Yaw, with vector observation aiding.

set to 5.0 arc-sec, while the body-referenced vector measurements were simulated to be acquired by a low accuracy attitude sensor with a noise equivalent angle of 0.1 deg. These measurements corresponded to a randomly selected vector, which was kept constant throughout the run.

The angular rates of the satellite satisfied $\omega_i(t) = A_i \sin((2\pi/T_i)t + \phi_i)$, where the amplitudes A_i are 0.02, 0.05, and 0.03 deg/s, the phases ϕ_i are $\pi/4$, $\pi/2$, and $3\pi/4$ rad, and the periods T_i are 85, 45, and 65 s for $i = 1,2,3$, respectively. The initial angular rate estimates were all set to zero. The true initial attitude corresponded to Euler angles of 30 deg, 20 deg, and 10 deg in roll, pitch, and yaw, respectively, while the initial state of the filter corresponded to Euler angles of 25 deg, 15 deg, and 5 deg, respectively. The filter was run at a rate of 20 Hz, and the measurement processing rate was 10 Hz. The Singer angular acceleration model was used with parameters set to $\tau = 10$ s, $\dot{\omega}_M = 10^{-4}$ rad/s^2, $p_M = p_0 = 0.001$ for all three axes.

In Fig. 2, the three true Euler angles are shown for a typical run. These angles were computed from the true attitude matrix assuming a 3-2-1 angle sequence. The Euler angle estimation errors, computed from the estimated attitude matrix assuming a 3-2-1 Euler angle sequence, are shown in Fig. 3. Fig. 4 presents the angular rates estimation errors for the same run, with and without vector measurement aiding. The mean and standard deviation of the estimation errors

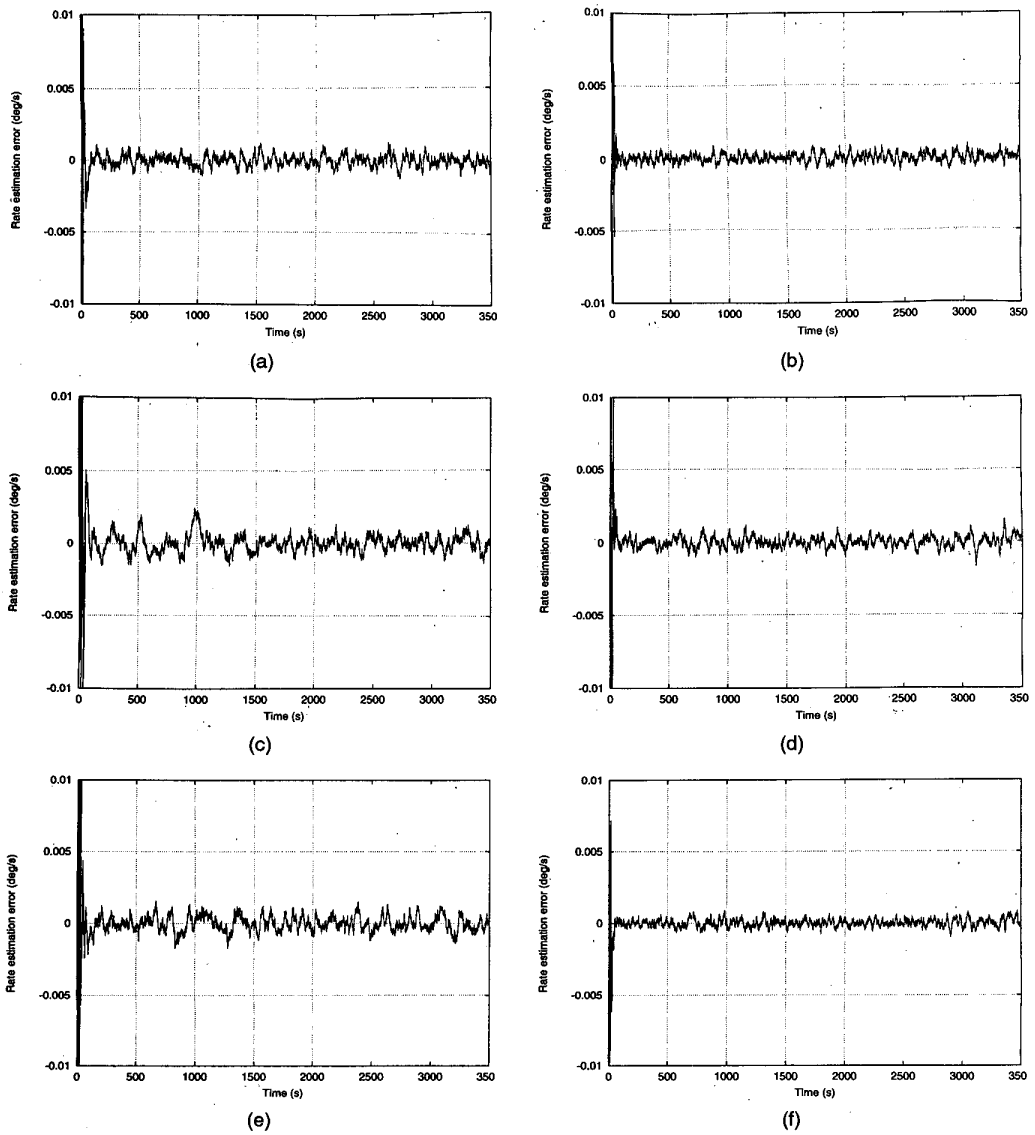

Fig. 7. Example II: Effect of vector observation aiding on angular rate estimation. (a) ω_1, GPS only. (b) ω_1, with vector observation aiding. (c) ω_2, GPS only. (d) ω_2, with vector observation aiding. (e) ω_3, GPS only. (f) ω_3, with vector observation aiding.

are summarized in Table I, which demonstrates the effect of the vector observation aiding in reducing the estimation errors standard deviation.

B. Example II

In this example, the same parameters were used as in Example I, except for the following. The three baselines used are now $\overline{b}_1 = [0.1, 1.0, 0.1]^T$, $\overline{b}_2 = [0.0, 1.0, 0.0]^T$, $\overline{b}_3 = [0.0, 0.0, 1.0]^T$. As can be observed, the first two baselines are almost colinear. The angular velocity of the satellite is $\omega = [0, 236, 0]^T$ deg/hr, which is typical for an Earth-pointing, low Earth orbit satellite, with pitch rate of one revolution per orbit. The Singer angular acceleration model parameters are set to $\tau = 10$ s, $\dot{\omega}_M = 10^{-5}$ rad/s^2, $p_M = p_0 = 0.001$ for all three axes. As in the first example, vector measurements, when available, correspond to a randomly selected vector, which is kept constant throughout the run.

In Fig. 5, the three true Euler angles are shown for a typical run. Fig. 6 shows the Euler angle estimation errors (the estimated angles were computed from the estimated attitude matrix assuming a 3-2-1 Euler angle sequence). Fig. 7 presents the angular rates estimation errors for the same run, with and without vector measurement aiding. The estimation error statistics are presented in Table II. As can be observed, especially from Fig. 6 and Table II, the robustifying effect of aiding the GPS measurements with vector observations is very significant in this ill-conditioned case.

TABLE I
Example I: Effect of Vector Observation Aiding on Estimation Performance

	GPS Only		Vector Observation Aiding	
Error	Mean	Standard Deviation	Mean	Standard Deviation
Roll angle (deg)	-9.2×10^{-4}	5.8×10^{-2}	-4.2×10^{-3}	3.9×10^{-2}
Pitch angle (deg)	3.0×10^{-3}	8.1×10^{-2}	-1.4×10^{-3}	2.2×10^{-2}
Yaw angle (deg)	7.1×10^{-3}	9.5×10^{-2}	9.9×10^{-4}	2.2×10^{-2}
ω_1 (deg/s)	-5.8×10^{-4}	9.5×10^{-3}	5.1×10^{-5}	8.2×10^{-3}
ω_2 (deg/s)	2.0×10^{-4}	2.7×10^{-2}	-2.8×10^{-4}	1.2×10^{-2}
ω_3 (deg/s)	4.0×10^{-5}	1.5×10^{-2}	3.9×10^{-4}	6.5×10^{-3}

TABLE II
Example II: Effect of Vector Observation Aiding on Estimation Performance

	GPS Only		Vector Observation Aiding	
Error	Mean	Standard Deviation	Mean	Standard Deviation
Roll angle (deg)	7.2×10^{-3}	6.4×10^{-2}	1.3×10^{-3}	2.0×10^{-2}
Pitch angle (deg)	1.1×10^{-3}	3.8×10^{-2}	-4.8×10^{-4}	2.0×10^{-2}
Yaw angle (deg)	7.7×10^{-3}	8.7×10^{-2}	4.6×10^{-3}	2.2×10^{-2}
ω_1 (deg/s)	-9.6×10^{-6}	4.8×10^{-4}	2.5×10^{-6}	3.3×10^{-4}
ω_2 (deg/s)	2.8×10^{-5}	9.9×10^{-4}	3.7×10^{-5}	5.1×10^{-4}
ω_3 (deg/s)	3.4×10^{-6}	9.3×10^{-4}	-5.8×10^{-6}	3.5×10^{-4}

VIII. CONCLUSIONS

A nonlinear sequential estimator has been presented, that uses differential GPS carrier phase measurements to estimate both the attitude matrix and the angular velocity of a spacecraft. The algorithm is based on the IRP third-order minimal parametrization of the attitude matrix, which is at the heart of its computational efficiency. Avoiding the use of the typically uncertain (and frequently unknown) spacecraft dynamic model, the filter uses a polynomial state space model, in which the spacecraft angular acceleration is modeled as an exponentially autocorrelated stochastic process. When vector observations are available (e.g., from low accuracy Sun sensors or magnetometers), the structure of the estimator can be easily modified to exploit this additional information and, thereby, significantly enhance the robustness and accuracy of the algorithm. Numerical examples have been presented, that demonstrate the performance of the proposed algorithm and the advantages of aiding the GPS carrier phase signals with vector observations, even when the vector measurements are of relatively low accuracy.

REFERENCES

[1] Cohen, C. E. (1996)
Attitude determination.
In B. W. Parkinson and J. J. Spilker, Eds., *Global Positioning System: Theory and Applications*, Vol. II.
Washington, DC: AIAA, Progress in Astronautics and Aeronautics, 1996.

[2] Crassidis, J. L., and Markley, F. L. (1997)
Attitude determination using Global Positioning System signals.
In *Proceedings of the AIAA Guidance, Navigation and Control Conference*, New Orleans, LA, Aug. 1997, pp. 23–31.

[3] Bar-Itzhack, I. Y., Montgomery, P. Y., and Garrick, J. C. (1997)
Algorithms for attitude determination using GPS.
In *Proceedings of the AIAA Guidance, Navigation and Control Conference*, New Orleans, LA, Aug. 1997, pp. 841–851.

[4] Fujikawa, S. J., and Zimbelman, D. F. (1995)
Spacecraft attitude determination by Kalman filtering of Global Positioning System signals.
Journal of Guidance, Control, and Dynamics, **18**, 6 (Nov.–Dec. 1995), 1365–1371.

[5] Axelrad, P., and Ward, L. M. (1996)
Spacecraft attitude estimation using the Global Positioning system: Methodology and results for RADCAL.
Journal of Guidance, Control, and Dynamics, **19**, 6 (Nov.–Dec. 1996), 1201–1209.

[6] Lefferts, E. J., and Markley, F. L. (1976)
Dynamic modeling for attitude determination.
In *Proceedings of the AIAA Guidance and Control Conference*, San Diego, CA, Aug. 1976, paper 76-1910.

[7] Merhav, S. (1996)
Aerospace Sensor Systems and Applications.
New York: Springer, 1996.

[8] Ronen, M., and Oshman, Y. (1997)
A third-order, minimal-parameter solution of the orthogonal matrix differential equation.
Journal of Guidance, Control, and Dynamics, **20**, 3 (May–June 1997), 516–521.

[9] Singer, R. A. (1970)
Estimating optimal tracking filter performance for manned maneuvering targets.
IEEE Transactions on Aerospace and Electronic Systems, **AES-6**, 4 (July 1970), 473–483.

[10] Wertz, J. R. (Ed.) (1978)
Spacecraft Attitude Determination and Control.
Dordrecht, Holland: D. Reidel, 1978, ch. 13.

[11] Oshman, Y., and Markley, F. L. (1998)
Sequential gyroless attitude/attitude-rate estimation using integrated-rate parameters.
In *Proceedings of the AIAA Guidance, Navigation and Control Conference*, Boston, MA, Aug. 1998; AIAA Paper 98-4508.

[12] Crassidis, J. L., Markley, F. L., and Lightsey, E. G. (1998)
Optimal integer resolution for attitude determination using Global Positioning System signals.
In *Proceedings of the AAS/GSFC 13th International Symposium on Space Flight Dynamics*, NASA Gosddard Space Flight Center, Greenbelt, MD, May 1998.

[13] Maybeck, P. S. (1979)
Stochastic Models, Estimation and Control, Vol. 1.
New York: Academic Press, 1979.

[14] Golub, G. H., and Van Loan, C. F. (1983)
Matrix Computations.
Baltimore, MD: The Johns Hopkins University Press, 1983.

[15] Markley, F. L. (1988)
Attitude determination using vector observations and the singular value decomposition.
The Journal of the Astronautical Sciences, **36**, 3 (July–Sept. 1988), 245–258.

[16] Bar-Itzhack, I. Y., and Meyer, J. (1976)
On the convergence of iterative orthogonalization processes.
IEEE Transactions on Aerospace and Electronic Systems, **AES-12**, 2 (Mar. 1976), 146–151.

[17] Oshman, Y., and Markley, F. L. (1997)
Minimal-parameter attitude matrix estimation from vector observations.
In *Proceedings of the AIAA Guidance, Navigation and Control Conference*, New Orleans, LA, Aug. 1997, pp. 12–22; AIAA paper 97-3451.

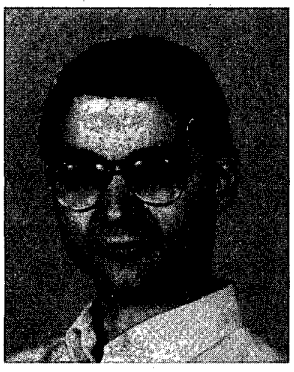

Yaakov Oshman (A'96—SM'97) received the B.Sc. (summa cum laude) and the D.Sc. degrees, both in aeronautical engineering, from the Technion–Israel Institute of Technology, Haifa, Israel, in 1975 and 1986, respectively.

From 1975 to 1981 he was with the Israeli Air Force, where he worked in the areas of structural dynamics and flutter analysis and flight testing. In 1987 he was a Research Associate at the Department of Mechanical and Aerospace Engineering at the State University of New York at Buffalo, where he was, in 1988, a Visiting Professor. Since 1989 he has been with the Department of Aerospace Engineering at the Technion–Israel Institute of Technology, where he is currently an Associate Professor. During the 1996/1997 and 1997/1998 academic years he spent a sabbatical with the Guidance, Navigation and Control Center of NASA's Goddard Space Flight Center, where he worked in research and development of spacecraft attitude estimation algorithms. His research interests are in advanced optimal estimation and control methods and their application in aerospace systems.

Dr. Oshman is an Associate Fellow of the AIAA.

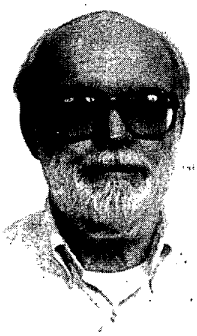

F. Landis Markley received the B.A. of engineering physics degree from Cornell University, Ithaca, NY, in 1962 and the Ph.D. in physics from the University of California, Berkeley, in 1967.

Following previous positions at Computer Sciences Corporation and the United States Naval Research Laboratory, he joined NASA's Goddard Space Flight Center in 1985. He has developed attitude determination and control algorithms for several NASA missions, including Solar Maximum Mission (SMM), Solar, Anomalous, and Magnetospheric Particle Explorer (SAMPEX), Tropical Rainfall Measuring Mission (TRMM), Rossi X-Ray Timing Explorer (RXTE), Compton Gamma Ray Observatory (CGRO), Hubble Space Telescope (HST), and Microwave Anisotropy Probe (MAP).

Dr. Markley is a member of the American Astronautical Society and SIAM, and a fellow of AIAA.